



HAL
open science

Very high-density planets: a possible remnant of gas giants

A. Mocquet, Olivier Grasset, C. Sotin

► To cite this version:

A. Mocquet, Olivier Grasset, C. Sotin. Very high-density planets: a possible remnant of gas giants. *Philosophical Transactions of the Royal Society A: Mathematical, Physical and Engineering Sciences*, 2014, 372 (2014), pp.20130164. <10.1098/rsta.2013.0164>. <hal-03160961>

HAL Id: hal-03160961

<https://hal.science/hal-03160961v1>

Submitted on 5 Mar 2021

HAL is a multi-disciplinary open access archive for the deposit and dissemination of scientific research documents, whether they are published or not. The documents may come from teaching and research institutions in France or abroad, or from public or private research centers.

L'archive ouverte pluridisciplinaire **HAL**, est destinée au dépôt et à la diffusion de documents scientifiques de niveau recherche, publiés ou non, émanant des établissements d'enseignement et de recherche français ou étrangers, des laboratoires publics ou privés.



HAL Authorization

Accepted version of

Mocquet, A., Grasset, O., Sotin, C., Very high-density planets : A possible remnant of gas giants,

Phil. Trans. R. Soc. A, 372: 20130164, 2014. doi:10.1098/rsta.2013.0164

Very high-density planets – a possible remnant of gas giants

Mocquet A.¹, Grasset O.¹, Sotin C.²

1. LPG-Nantes, UMR-CNRS 6112, Nantes university, France

2. Jet Propulsion Laboratory, Pasadena, US

Corresponding author: Olivier Grasset, LPG-Nantes, 2 rue de la Houssinière, 44322 Nantes Cedex 03, France. Email: olivier.grasset@univ-nantes.fr

Abstract: Data extracted from the Extrasolar Planets Encyclopaedia [1] show the existence of planets that are more massive than iron cores that would have the same size. After meticulous verification of the data, we conclude that the mass of the smallest of these planets is actually not known. However, the three largest planets Kepler-52b, Kepler-52c, and Kepler-57b, which are between 30 and 100 times the Earth mass, have indeed density larger than an iron planet of the same size. This observation triggers the present study that investigates under which conditions these planets could represent the naked cores of gas giants that would have lost their atmospheres during their migration towards the star. This study shows that for moderate viscosity values (10^{25} Pa.s or lower), large values of escape rate and associated unloading stress rate during the atmospheric loss process, lead to the explosion of extremely massive planets. However, for moderate escape rate, the bulk viscosity and finite strain incompressibility of the cores of giant planets can be large enough to retain a very high density during geological timescales. This would make those planets a new kind of planets, which would help understand the interior structure of the gas giants. However, this new family of exoplanets adds some degeneracy for characterizing terrestrial exoplanets.

I. Introduction

Mass – Radius (M-R) relations for low mass planets have been extensively studied in the last decade. Following the pioneering approach of [2], who studied planetary M-R relations assuming homogeneous spheres, many authors have investigated the internal structure of more complex bodies, relevant to the super-Earths family (see, e.g., [3-6]). These studies used a complex chemistry for silicates and also introduced thermal effects in addition to pressure effects on the density of solid materials. Water was also added to the models in order to explore the M-R relationships for water-rich planets [3]. Seager et al. [7] also described carbon-rich planets, in addition to cold planets made primarily of iron, silicates, and water. Grasset et al. [8] proposed a review of the different approaches for planetary masses up to 100 Earth mass (M_E), which concluded that a general agreement is found among the different models for each planetary family. A few minor discrepancies were noticed, mostly explained by the fact that models use different temperature fields, different modal compositions for silicates, and different equations of state. In Figure 1, the different estimates of M-R relationships based on these previous studies in the range 1-100 M_E have been plotted. The four curves represent the M-R relationship for H₂O planets, Ocean planets (50% H₂O, 50% silicates), Earth-like planets, and Mercury-like (almost pure iron) planets.

For a given mass, the size of a gaseous planet is roughly three times as large as a terrestrial planet. Mercury-like planets, mostly composed of iron, are about 20 % smaller than Earth-like planets (Figure 1). The radii also strongly depend on the amount of ices which can be determined only if mass and radius are well known [8]. Indeed, all the uncertainties related to the unknown temperature, exact composition, and chosen equation of state remain small compared to the effect of the low density of ices on the value of the radius for a given mass. But this is only true if the atmospheric contribution is negligible. Indeed, a silicate-rich planet

surrounded by a very thick atmosphere could provide the same mass and radius than an ice-rich planet without atmosphere [9,10]. The existence of this thick atmosphere can be explained either by an important outgassing during the planet history or by an erosion of a massive primordial atmosphere mostly composed of hydrogen and helium. That is why all planets discovered in the domain from iron-rich to water-rich planets cannot be characterised properly for the time being, even if mass and radius are accurately measured. As long as there is no way to determine the nature and abundance of its atmosphere, the solution cannot be unique.

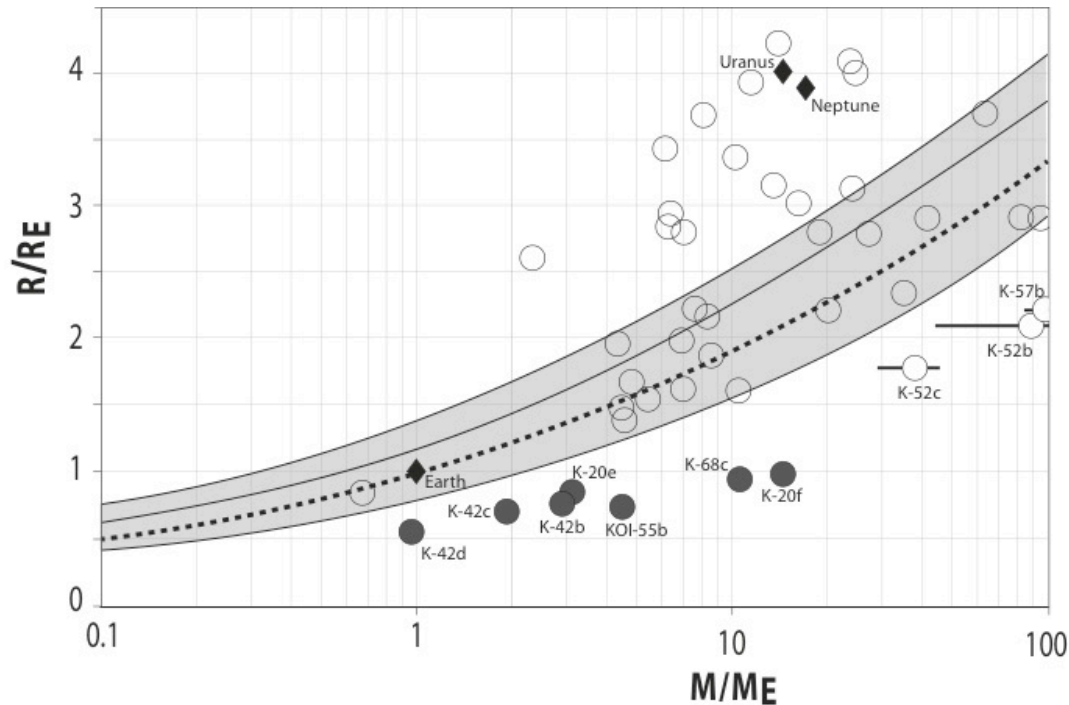


Figure 1: (Mass,Radius) for planets of less than 100 Earth-mass. The four curves are, in density increase from top to bottom, pure H_2O , ocean planets (50% H_2O , 50% silicates), Earth-like (dashed and bold), pure iron. The nature of the planets located in the shaded area cannot be determined accurately without any information regarding the composition and/or the amount of the atmospheres [9]. Planets above must have an envelope of light gases H_2 and He. Planets below the iron curve are enigmatic and the focus of this study. E: Earth; U: Uranus; N: Neptune; White circles: planets with independent M-R estimates; Grey circles: planets for which the mass is still badly constrained and model-dependent. In the latter case, the position of the point corresponds to the densest case proposed in the literature.

More recently, Kepler's observations raised a new issue regarding the characterisation of Earth-like planets from M-R measurements. The Extrasolar Planets Encyclopaedia [1] provides the database used in this study. Planets with values of radius and mass lower than 100 Earth-mass have been extracted. Their masses and radii have been scaled to the Earth's values ($M_E=5.97 \cdot 10^{24}$ kg, $R_E=6371$ km), and plotted in Figure 1. Planets below the pure iron case are outliers that triggered that study since their nature is enigmatic. Two solutions are envisaged: either these outliers have one of their parameter wrongly reported, or they represent a new class of planet, the latter being clearly the most intriguing. Because they all are located very close to their star, this study investigates the possibility for these planets to be remnant cores of giant planets that evaporated their gaseous envelope during their migration toward the star. In such a process, the important timescales are the evaporation rate of the planet and the relaxation of the interior density. As pointed out in the study of KOI-55b, which is one of the very small planets of this new kind [11], "These bodies probably survived deep immersion in the former red-giant envelope. They may be the dense cores of evaporated giant planets that were transported closer to the star during the engulfment and triggered the mass loss necessary for the formation of

the hot B subdwarf, which might also explain how some stars of this type did not form in binary systems”.

Following the discovery of hot Jupiters, i.e. massive giant planets very close to their stars, it has been understood that giant planets that have formed far from their host stars can migrate inward in many cases. Since then, many models of planetary system evolution have been developed to investigate the migration processes that may have occurred in the stellar systems which host exoplanets [12,13]. Because we have many evidences in our galaxy that such processes are rather common, it has also been suggested that in some cases, a giant planet may come too close to its star and thus, lose a significant part of its atmosphere (see, e.g., [14-18]). In the following sections, we assume that such processes exist and may explain the origin of the dense planets discovered by Kepler. The idea of having naked cores of giant planets as potential members of the Super-Earth families has been already discussed in a few studies, especially for Earth-like bodies such as Corot-7b [19]. Our purpose here is to demonstrate that an incomplete decompression of the pre-strained naked core during the atmospheric escape, may explain the existence of very dense cores close to their stars. To illustrate the idea, one example is displayed in Figure 2. The two extreme cases corresponding to full relaxation or fossilized state of the inner core of an Uranus-like planet are displayed.

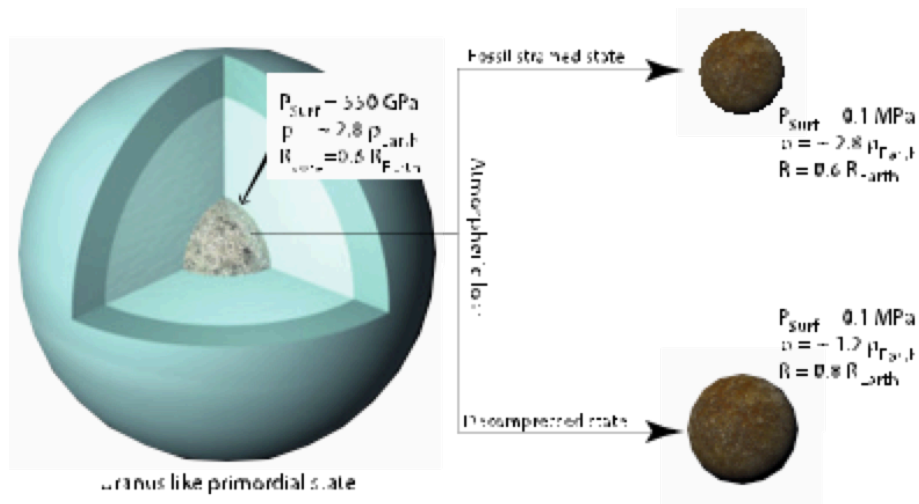


Figure 2: Two extreme scenarios after evaporation of the gaseous envelope of an Uranus-like planet. Assuming a core of 0.6 Earth mass and 0.6 Earth radius [36], the compressed state is such that the mean density of the rocky core is ~ 2.8 the times the Earth mean density value. In the fossilized state, the naked core remains much denser than its Earth analogue. In the second case where full decompression occurs, the remnant core can hardly be distinguished from the Earth.

In this study, a thorough analysis of the mass and radius estimates that have been provided for the very dense planets is achieved. The second part describes a preliminary analysis of a possible scenario that explains the origin and the stability of very dense objects. It is based on the estimated time needed to relax the massive core of a giant planet, if it were possible for its atmosphere to be expelled during its migration towards the star. This section summarizes an ongoing much more detailed study, and provides the proper order of magnitude for the estimate of the decompression process. In a last part, new M-R curves for very compressed remnant cores of giant planets are proposed and compared to the recent Kepler data.

II. Recent observation of very dense planets

Information on the radius and mass of exoplanets is extracted from the Extrasolar Planets Encyclopedia (Fig. 1). Ten exoplanets are located below the curve of Mercury-like planets. The density is calculated with the values of mass and radius provided in this database (Table 1). The very large values look suspicious leading us to question the information provided in the data

base. On the one hand, the radius of these ten planets is determined by transit observations and the values seem quite robust. On the other hand, the values for the mass are not that well known. Actually, the value of the mass is not known for the smallest planets. For the three largest ones (Kepler-52b, Kepler-52c, Kepler-57b), the value of the mass is inferred from observations of transit time variations (TTVs) that result from changes in the orbital period of the planets due to planet-planet interactions in multi-planet systems when the planets are near a mean-motion resonance [20]. It is important to note that the values for the masses are maximum values. The study by [21] uses an analytical solution that links the mass of the planets to the amplitude of the TTVs. The comparison to the N-body-simulated TTV is very good. However, their study does not provide the results for the Kepler-52 and Kepler-57 systems. Therefore the values reported in Table 1 are from [20].

Planet name	Mass estimate (/Earth)	Radius (/Earth)	Planet Period (day)	Semi-axis (AU)	Density (kg/m ³)	Reference
Kepler-42 d	0.95*	0.57	1.856169	0.0154	unknown	[24]
Kepler-42 c	1.91*	0.73	0.453285	0.0060	unknown	[24]
Kepler-42 b	2.86*	0.78	1.213767	0.0116	unknown	[24]
Kepler-20 e	3.08*	0.87	6.098493	0.0507	unknown	[25]
KOI-55 b	4.45*	0.76	0.2401	0.0060	unknown	[11]
Kepler-20 f	14.30*	1.03	19.57706	0.1100	unknown	[25]
Kepler-52 c	38.14	1.84	16.385	0.1028	36,341	[20]
Kepler-52 b	88.99	2.10	7.877357	0.0631	50,637	[20]
Kepler-57 b	98.53	2.19	5.72932	0.0589	48,067	[20]
Kepler-68 c	10.60*	0.95	9.605085	0.0906	unknown	[22]

Table 1: Characteristics of the ten exoplanets denser than iron balls. The mass of those planets is still unknown except for Kepler-52c, Kepler-52b, and Kepler-57b for which upper bounds are inferred from transit time variations. Mass estimates with a (*) are extracted from [1].

The Kepler-52 system consists of two planets orbiting a star near a 2:1 resonance [20]. The inner planet (Kepler-52b) is the most massive. The maximum mass of each planet provides a density much larger than the density of an iron planet that would have the same size (Figure 1). Their real masses should be about 5 times smaller to be on the terrestrial trend and 2 times smaller to be on the iron trend. The temperatures of a rapidly rotating black body at a similar distance of the star are equal to 563 K and 441 K for Kepler-52b and Kepler-52c, respectively. These values are larger than the 278 K value for the Earth.

The system Kepler-57 consists of two planets near a 2:1 resonance orbiting a star smaller than the Sun. Like the Kepler-52 system, the planet Kepler-57c is much smaller than Kepler-57b (R57c = 1.57 Earth radius) and orbits the star at a larger distance. Upper limits for the mass of the two planets were determined by using the transit time variations. The value for Kepler-57c lies on the terrestrial trend whereas the value for Kepler-57b is 3 and 5 times larger than the mass of an iron planet and a terrestrial planet, respectively. Compared to the Kepler-52 system, there is a very large difference in mass between the two planets. The temperature of a rapidly rotating black body at a similar distance of the star is equal to 872 K for Kepler-57b.

Future information on the Kepler-52 and Kepler-57 planets may show that those planets have a mass much smaller than the upper value inferred by the TTVs. Even if that turns to be the case, it is important to investigate how the solid part of a planet evolves during atmospheric escape since some exoplanets are thought to be the remnants of icy giants. For example, Kepler-68c could be an ice giant that lost most of its primordial H₂/He atmosphere [22]. The next section investigates the evolution of the solid part of a planet during atmospheric escape.

III. From giant planets to compressed cores – a preliminary analysis

III.1. The loss of planetary atmospheres

The time scale of the pressure unloading process is governed by the time that is necessary to erode a given atmospheric mass. Depending on the evolution of the emitted stellar radiation, on the possibly varying orbital distance, and on the composition and thermodynamic properties of the planet atmosphere, the escape may be governed by different processes, either energy-limited, diffusion-limited, or through blow-off (e.g., [23]). We consider the extreme case of energy-limited escape (e.g., [24]), where the atmospheric loss is proportional to the ratio between the incident flux of the stellar extreme ultraviolet radiation and the gravitational potential of the planet, corrected from the tidal interaction between the star and the planet [16,17]. The coefficient of proportionality depends on the atmospheric composition and heating efficiency. All these parameters are time-dependent. Valencia et al. [25] applied this model to the case of CoRoT-7b and found a mass loss $\sim 10^8 \text{ kg s}^{-1}$, in the upper range of values [10^2 kg s^{-1} – 10^9 kg s^{-1}] estimated by [18] for extrasolar planets. Valencia et al. [25] concluded that the CoRoT-7b value favored the possibility of a water vapor atmosphere instead of a Hydrogen-Helium envelope, which would escape in $\sim 1 \text{ Ga}$ and $\sim 1 \text{ Ma}$, respectively. If we consider extreme cases of evaporation rates, the latter durations correspond to mean incremental stresses in the range [10^5 Pa – 10^8 Pa] per year. For comparison, the upper bound of this range corresponds to the level of constant shear stresses associated with convection processes within the Earth's mantle. Here, we present the results obtained for three 1 Ga long cases (Figure 3).

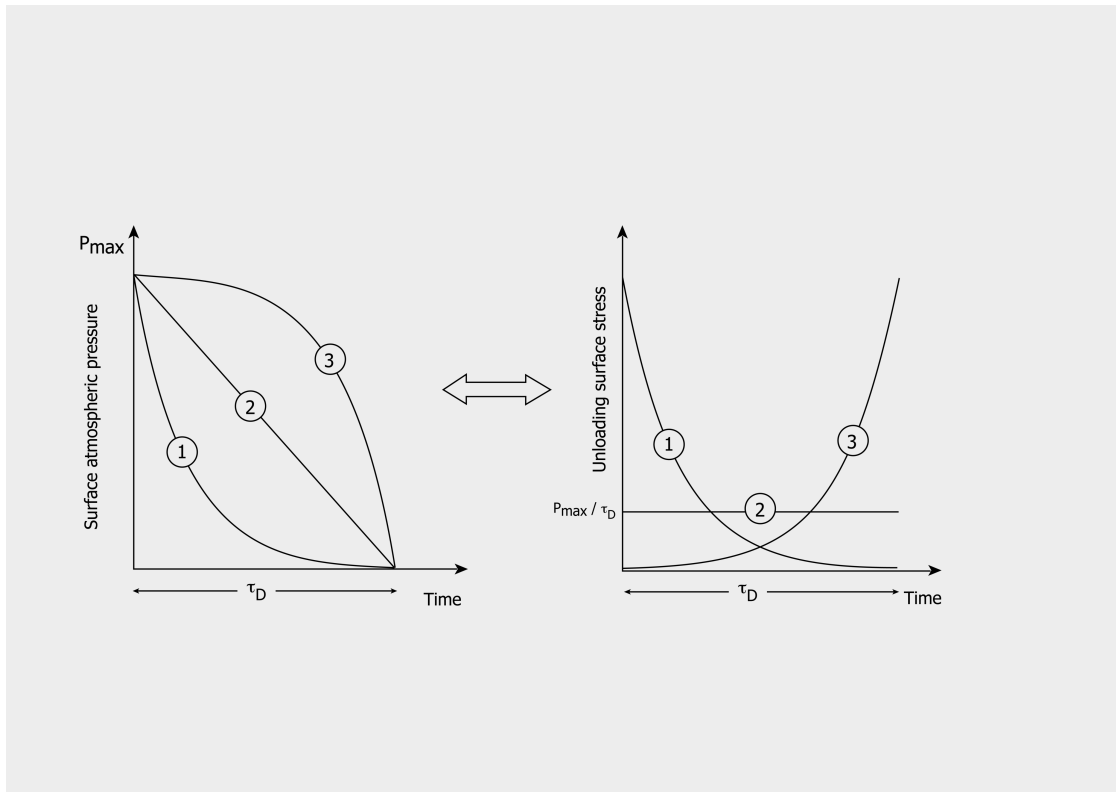


Figure 3. A sketch of the three unloading cases considered in this study. The temporal evolutions of the atmospheric pressure at the surface of the solid core, and the corresponding unloading stress histories are displayed in the left and right panels, respectively. P_{max} and τ_D are the initial pressure and duration of the atmospheric loss, respectively. In cases 1 and 3, the rate of pressure loss either decreases (case 1) or increases (3) with time. Case 2 corresponds to a constant pressure loss over time.

III.2. A simple model to quantify the relaxation of naked cores

Prior to atmospheric loss, the solid core of the planet is submitted to extremely high pressures and associated irreversible finite strains. When considering the instantaneous unloading stress levels and time scales, we choose to describe the solid core rheological response through a viscoelastic Maxwell rheology defined by three parameters: the incompressibility derived from equations of state, the viscosity, and the Poisson ratio. In the absence of information on the bulk viscosity, we assume that the Poisson ratios of elastic and viscous moduli are identical, which implies that the bulk viscosity amounts to twice the shear viscosity value. The behavior of the viscosity at the very high pressure and temperature conditions of extra-solar planets, is a current matter of debate. Stamenkovic et al. [26] used a semi-empirical homologous temperature approach to scale enthalpy variations with melting temperature, and to assess the very high pressure- and temperature-dependence of the viscosity. They obtained a factor of two reduction for the activation volume of Mg-perovskite between 25 GPa and 1.1 TPa, resulting in a viscosity increase by ~ 15 orders of magnitude through the adiabatic mantle of a $10 M_E$ planet. Their results contrast with Karato's [27] conclusions that viscosity should decrease with pressure when the later exceeds ~ 0.1 TPa. The advocated causes of this decrease are the transition from vacancy to interstitial diffusion at ~ 0.1 TPa, a phase transition in MgO at ~ 0.5 TPa, the dissociation of Mg-perovskite at ~ 1 TPa, and the transition to the metallic state in the same pressure range. Karato [27] concluded that, taken together, these phenomena lead to a significant decrease of the viscosity, by at least 2 or 3 orders of magnitude with respect to the maximum viscosity of the Earth's lower mantle. The possibility of a low-viscosity value would also be enhanced if some water exists in the solid planet [28] since first-principles molecular dynamics simulations have shown that the water-silicate system becomes increasingly ideal at high pressure [29]. The incorporation of ab-initio calculations in statistically steady-state numerical simulations of mantle convection with up to ten Earth masses, also leads to a self-regulation of temperature at very high pressure, through a feedback between internal heating, temperature, and viscosity [30]. These numerical experiments predict a $10^{25} - 10^{26}$ Pa.s range for the viscosity at very high pressure and temperature.

The Poisson ratio of silicates steadily increases with increasing pressure, with a value of ~ 0.3 at the base of the Earth's lower mantle, i.e. at ~ 0.15 TPa [31]. Within the metallic Earth's solid core, the ratio is of the order of 0.45 or higher, i.e. close to the incompressible value (0.5). Here, the calculations are performed using values of 10^{25} Pa.s and 0.3 for the viscosity and Poisson ratio, respectively, which allow for substantial volumetric strains.

The temporal evolution of the volumetric strain is computed using the procedure described by, e.g., [32]. The unloading stress histories described in the previous section are convolved with the impulse response of the solid core to a unit unloading radial stress applied on its surface at a given time t_s of the unloading stress function. By applying the correspondence principle between elastic and viscous deformations to the equation of motion in the Fourier-Laplace domain [33], and combining it with Poisson's equation, the radial displacement per unit stress $u_r(r_a)$, where r_a is the radius of the solid core at time t_s , is obtained by solving (e.g., [34])

$$\frac{d}{dr} \left[\frac{1}{r_a^2} \frac{d}{dr} \left(r_a^2 u_r \right) \right] + \frac{GM_c^2}{\pi K r_a^6} \left(\frac{1+\nu}{1-\nu} \right) u_r = 0 \quad (1)$$

where G is the gravitational constant, M_c is the mass of the solid core, and K^* is the complex incompressibility. For sake of simplicity, the spectral dependence of the displacement and complex incompressibility is not explicitly written in the equation. The surface radius and

internal pressure of the solid core, and the corresponding incompressibility, are actualized at each source time step.

The solutions of equation (1) are proportional to the spherical Bessel functions of the first kind $j_0(\gamma r_a)$ and $j_1(\gamma r_a)$

$$u_r \propto j_1(\gamma r_a) \quad ; \gamma = \frac{M_c}{r_a^3} \sqrt{\frac{G}{\pi K} \left(\frac{1+\nu}{1-\nu} \right)} \quad (2a)$$

$$\sigma_{rr} \propto 3K \left[\frac{(1-\nu)}{(1+\nu)} \gamma j_0(\gamma r_a) - \frac{2(1-2\nu)}{r_a(1-\nu)} j_1(\gamma r_a) \right] \quad (2b)$$

with the boundary condition $\sigma_{rr}(r_a) = 1$ at the surface of the solid core. The impulse response is transformed back to the time domain prior convolution, and the final radius at time t is given by

$$r_d(t) = r_d(0) + \int_0^{\tau_D} \sigma_S(\tau) \left[u_r(t-\tau) \right]_{r_d(\tau), K(\tau)} d\tau \quad (3)$$

where $r_a(0)$ is the outer radius of the planet at the onset of atmospheric loss, and σ_D is the time-dependent unloading stress. We consider that the finite-strain elastic deformation is also irreversible and set $r_a(t > \tau_D) = r_a(\tau_D)$. The volumetric strain at time t is calculated according to

$$\varepsilon_V(t) = \left[\frac{r_d(t)}{r_d(0)} \right]^3 - 1 \quad (4)$$

Examples of temporal evolutions are displayed in Figure 4 for Uranus- and Neptune-like planets, and for extremely massive exoplanets like K-52b, K-52c, and K-57b. Whatever the scenario of atmospheric pressure unloading, Uranus- and Neptune-like planets, with initial surface pressures of the order of 550 GPa, do not suffer volumetric strains larger than 20%. Due to gravity, the deformation of Neptune is smaller than the deformation of the less massive Uranus. For extremely high pressures, the unloading stress scenario plays a key role in the temporal evolution of the strain, potentially leading to a loss of cohesion of the planet if the rate of atmospheric loss is too high (see cases 1 and 3 in Figures 3 and 4). These results suggest that large planetary cores may stay in an incompletely relaxed state for billions of years, provided that their mass and viscoelastic incompressibility are able to counteract a given level of unloading stress rate. Note however that these preliminary results were obtained for homogeneous spheres with depth-independent rheological values that scale, at each time step, with the time-dependent mean pressure of the planet interior. If the radial rheological stratification of the planet were taken into account, it is expected that the stiff behavior of the high viscosity uppermost layers should result into brittle deformations over a still unknown depth range, even in case 2. These calculations will have to be incorporated into more elaborated studies.

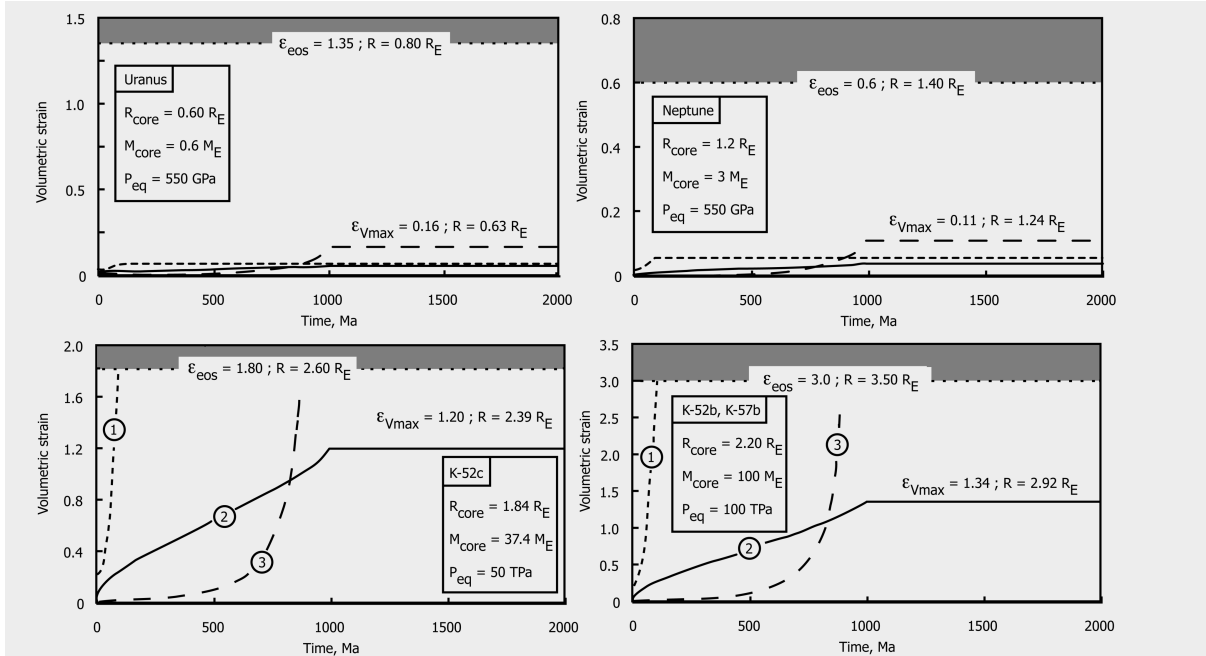


Figure 4. The temporal evolution of the volumetric strain induced by the three atmospheric unloading scenarii displayed in Figure 3. Results are shown for Uranus- and Neptune-like planets (top panels), and for the extremely massive exoplanets K-52b, K-52c, and K-57b (bottom panels). In all these examples, atmospheric loss is considered to be completed after $\tau_D = 1$ Ga. R_E and M_E refer to Earth's outer radius and solid mass, respectively; P_{eq} is the surface pressure equivalent to the initial atmospheric mass; ϵ_{eos} and associated outer radius correspond to the completely relaxed values expected from equations of state at $P_{eq} = 10^5$ Pa. The cohesion of the planet is lost for volumetric strains larger than ϵ_{eos} (gray shaded areas).

IV. Mass-radius relationships for compressed cores

IV. 1 Composition of the compressed cores

In this preliminary study, massive core of giant planets are supposed to be fully differentiated and composed of an iron rich core and a thick silicate layer. Sotin et al. [6] have shown that a rocky planet can be described using only four elements (Si, Mg, Fe, O) and adding (Ca, Al, Ni, S) to their closest major element. No water layer is considered in this study. First, we argue that any icy mantle should have vaporized into space - we are studying very dense objects. Additional water could also have been stored in silicates in the early stages of the planet history. On Earth, the amount of water trapped in the upper mantle is very small and still debated [35], but in any case it is less than 0.25 % of the planetary mass. It is envisaged that a larger amount of water may have been stored in the silicates at very high pressures [29]. It influences the viscous behaviour of the mantle, but it cannot be considered as major factor for M-R relationships, as it has already been demonstrated for Earth-like planets [6].

In all results hereafter, the composition of the planets is based on stellar abundances but taking into account the contribution of secondary compounds in their major counterparts ($[Fe/Si]=0.977$ and $[Mg/Si] = 1.072$). In order to get these numbers, it is assumed that Ni behaves like Fe, sulphur is added to iron, Al is equally divided between Mg and Si, and Ca is added to Mg (see [6]). Distribution of the four chemical compounds (Si, Mg, Fe, O) between the silicate mantle and the iron core is unknown. Magnesium can only be incorporated in silicates, while iron, oxygen, and silicium can be distributed either in silicates or in the metallic core. Following [26], we propose a simplified mineralogy: the mantle is composed of the Mg end-

member for the perovskite or post-perovskite phase and of pure magnesowüstite (MgO). Consequently, all the iron is contained in the core, which is assumed pure and homogeneous. These crude assumptions have little impact on the (M-R) values. Using a Monte Carlo simulation, Grasset et al. [8] showed that M-R relationships strongly depend on the amount of water and atmosphere and weakly depend on parameters such as the distribution of iron between core and mantle, temperature profile, and bulk composition of the planet.

Our model is based on a previous version described in details in [6] and extended to large masses above $10 M_E$ in [8]. One key issue of this model is the choice of the equations of state for each material, that is the relation between temperature, pressure, and density. In the silicate mantle, we use the Keane formulation for the equation of state, as described in [26] for very high pressures. Since this paper is dealing with compressed planets for which no low-pressure silicates should be considered, this formulation is the most appropriate for silicates. In addition, the reference case comparable to the Earth-like planets uses the Birch-Murnaghan equation of state for the upper mantle. As for the iron core, a Keane's formulation might certainly be used but to our knowledge, there are no published parameters. That is why a Mie-Grüneisen-Debye formulation has been chosen to describe the entire core. Grasset et al. [8] have shown that this equation of state, commonly used in Earth sciences, provides comparable results to both ANEOS and Thomas-Fermi-Dirac formulations up to a few tens of TPa.

IV.2 Description of the results

In figure 5, four curves are plotted for equivalent surface pressures of 0.1 MPa (Earth's ambient pressure), 500 GPa, 1 TPa, 10 TPa, and 100 TPa respectively. This pressure should be considered as the pressure needed for the surface material to be in equilibrium state. All surface materials are under negligible pressures, but since they have had no time to relax entirely, they must be at a much higher density than the density at low pressure. The equivalent surface pressure corresponds to the pressure needed for getting this high density. As an example, the rocky cores of Uranus and Neptune as described in [36] are plotted with black circles. In one of their models, mass and radius of the core of Uranus are $0.6 M_E$ and $0.6 R_E$, respectively. As for Neptune, the mass is $3 M_E$ and the radius is $1.2 R_E$. For both planets, the pressure at the interface between the core and the outer envelopes is about 550 GPa. If for such bodies one imagine that the outer envelopes are expelled and that relaxation is weak (top panels of Figure 4), we should still see these bodies close to the 550 GPa curve. These two points in Figure 5 also confirm that our results are consistent with [36] regarding the internal structure of very compressed rocky cores.

The nine exoplanets that have been explored in details in section 1 are also plotted in Figure 5, together with the less dense planets of the Super-Earth family. One result of this study is that there is indeed a way to reproduce the very dense nature of these peculiar planets. From left to right, the mean density of planets varies from $5,000 \text{ kg/m}^3$ to $15,000 \text{ kg/m}^3$ along the 0.1 MPa curve, but it goes from $53,000 \text{ kg/m}^3$ up to $59,000 \text{ kg/m}^3$ at 100 TPa. Such dense bodies have no equivalent in our Solar System and must be considered as totally new objects which open new perspectives regarding the nature of the "super-Earths" candidates. On the other hand, one must keep in mind that the equivalent pressures needed for getting such bodies are extremely high. So far, current models estimate that the pressure at the surface of Jupiter's core should be about 4 TPa. How big must be a planet for which the inner pressure could attain 100 TPa? To answer this question is out of the scope of this paper, but is worth considering for future studies.

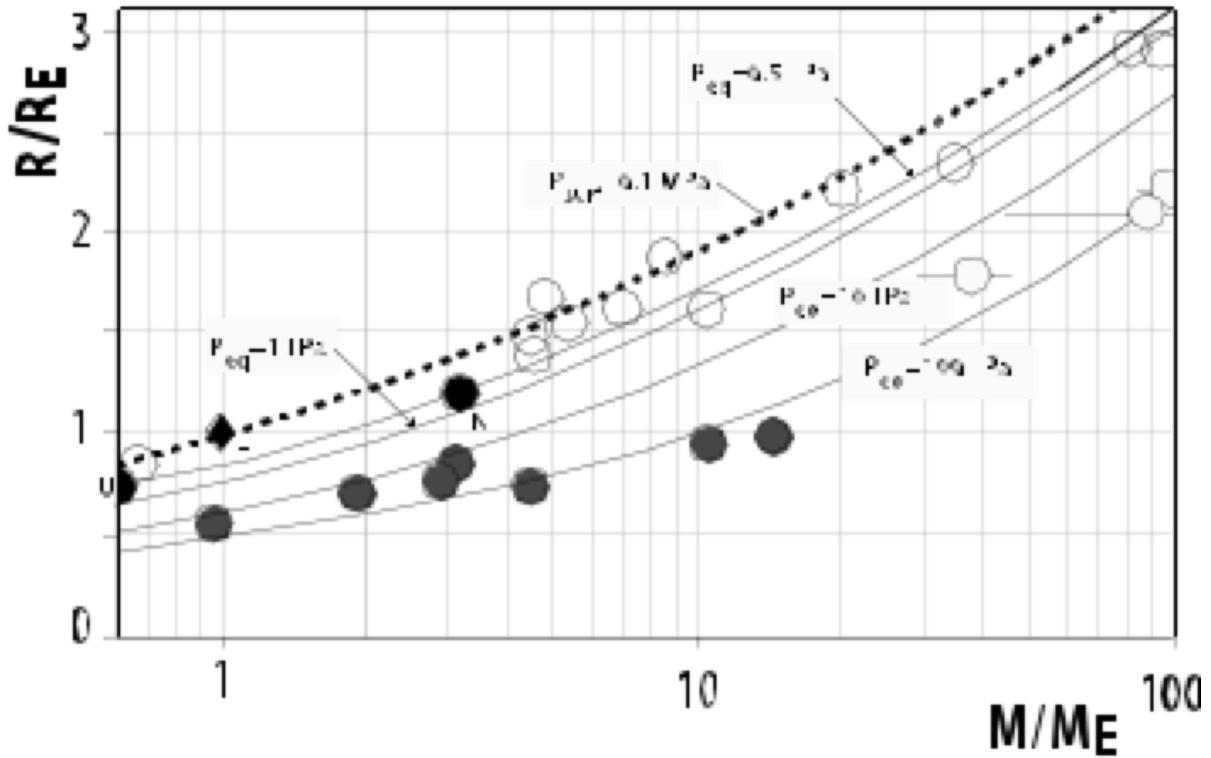


Figure 5: Mass radius relationships for naked cores of gaseous planets. Five curves are plotted as a function of the surface equivalent pressure (see text for details – the upper dashed and bold curve is for Earth-like planets). Similarly to Figure 1, grey dots are used for possibly super-dense planets for which the mass is actually unknown. Black dots correspond to the putative naked cores of Uranus (U) and Neptune (N) from [36].

V. Discussion and conclusion

Super-Earths are one of the most important targets of space exploration for the next decades. With the discovery of potential candidates that suggests a high probability for having other Earths in our galaxy, it is important to ascertain how confident we can be that a planet with adequate mass and radius is indeed like our Earth's planet. It has already been shown in previous studies that similar mass and radius relationships can be found for Super-Earths and mini-Neptune. In this paper, we propose that a third family should also be considered. Since planetary migration is a common process in stellar systems, it is highly possible that a few “planets” discovered close to their stars are in fact the remnants of the inner core of gaseous exoplanets. Relaxation processes and mass-radius relationships of highly compressed rocky cores of giant planets after vaporization of the outer layers have been investigated. It has been shown that the very dense objects discovered recently by Kepler might be such bodies, provided that atmospheric escape rates are low over Ga time scales. Another important result of this study is that the cohesion of a planet is lost when the atmosphere escapes quickly.

In this work, gaseous planets have been supposed to be made of one or several envelopes of volatiles (including water) and a core composed of rocks and iron. This crude assumption is rather in agreement with what is commonly accepted to be the internal structure of Uranus-like and Neptune-like planets. It is especially in agreement with the model proposed by [36] for Uranus and Neptune. But evidences of very dense and very massive planets indicate that it is the cores of gaseous giants such as Jupiter that should be considered in some cases (see Kepler-52b, 52c, and Kepler-57b). Nonetheless, it is not clear whether giant gaseous planets possess a dense core. For Jupiter, a few models have already shown that internal structures without a solid core are still consistent with the available data (see [37]). It is out of the scope of this study to analyse

the different models that describe the inner structure of Jupiter-like planets. But it is worth noting that very dense planets such as Kepler-52b,c and Kepler-57b may be seen as the first evidences of solid cores of giants planets. Now, it must be understood that this possibility arises new difficulties. For the three dense exoplanets (Kepler 52b, 52c, and 57b), it can be seen in Figure 5 that the pressure at the top of the core before envelope evaporation must had been above 50-100 TPa, meaning that the primordial planets were extremely massive. If one assumes hydrostatic equilibrium in the envelope and homogeneous density, the central pressure can be expressed as $3GM^2/(8\pi R^4)$. Of course, this equation underestimates pressure by a factor of at least two, but it indicates that the total mass of the primordial exoplanet before evaporation is well above the minimum mass for brown dwarfs (13 times the mass of Jupiter).

One finding of the present study is that there is no reversibility between accretion during which the core is rapidly compressed, and evaporation that expels the outer layers once the planet is close to its star. The different time scales that are involved in both processes may be understood by inverting the temporal evolution of scenario 1 in Figure 4. If one considers compressional instead of extensional stresses, high compression rates can be explained by the high-rate loading of low-pressure and compressible rocks. Furthermore, the percolation of liquid iron towards the center of the planet favors high compression rates. On the other hand, during a low-rate atmospheric escape (scenario 2 in Figure 4), the incompressibility of planetary materials already in a very-high pressure finite strained state is much higher and the extensive relaxation of the planet occurs slowly.

In the Uranus- and Neptune-like cases displayed in figure 4, unloading stress levels are sufficiently low that the final volumetric strain merely depends on the decompression path. For extremely high stress levels, escape rates play a key role in the decompression history, even for very massive planets such as the Kepler objects, and the decompressed state is strongly dependent on the age of the planet. The older the planetary system is, the larger the decompression of naked cores should be. This must be taken into account if one wants to study a very dense object. A careful study of the nature of these small objects, potentially still away from equilibrium, requires the age of the system to be known. Also, a planet so close to its star that its surface temperature is very high may reach the new gravitational equilibrium much quicker since the viscosity is very much temperature dependent.

This study is a brief overview of a very complex problem, i.e. the quantification of the relaxation processes of an entire planet as a function of its orbital evolution. No doubt that Kepler's discoveries widen the field of possibilities regarding the origin of the dense planets since they may be the proof that exoplanetary small planets could be either a "real" terrestrial planet or a remnant of giant planet for which the final state depends on the migration processes leading to the evaporation of outer layers. Detailed studies on these very dense objects that have been discovered by Kepler will be needed before any determination of their exact nature can be made. Additional parameters to mass and radius, such as their age, their distance to the star, or the bulk composition of the system will have to be incorporated in future models to confirm that we may be observing the fossilized cores of giant exoplanets. This first study strongly suggests that such occurrences are indeed possible.

Acknowledgments:

Part of this work was performed at the Jet Propulsion Laboratory (Caltech) under contract with NASA. The constructive comments of two reviewers were very helpful to improve a first draft of this paper.

References:

[1] Extrasolar Planets Encyclopaedia. See <http://exoplanet.eu>

- [2] Zepolsky, H. S. & Salpeter, E. E. 1969 The Mass-Radius relation for cold spheres of low mass. *ApJ*. **158**, 809-&. (DOI 10.1086/150240)
- [3] Léger, A. & 11 co-authors 2004 A new family of planets ? « Ocean-Planets ». *Icarus* **169**, 499-504. (DOI 10.1016/j.icarus.2004.01.001)
- [4] Valencia, D., O'Connell R. J. & Sasselov, D. 2006 Internal structure of Earth-like planets. *Icarus* **181**, 545-554. (DOI 10.1016/j.icarus.2005.11.021)
- [5] Valencia, D., Sasselov, D. D. & O'Connell, R. J. 2007 Detailed models of super-Earths: How well can we infer bulk properties? *ApJ*. **665**, 1413-1420. (DOI 10.1086/519554)
- [6] Sotin, C., Grasset, O. & Mocquet, A. 2007 Curve mass/radius for extrasolar Earth-like planets and ocean planets. *Icarus* **191**, 337-351. (DOI 10.1016/j.icarus.2007.04.006)
- [7] Seager, S., Kuchner, M., Hier-Majumder, C. A. & Militzer, B. 2007 Mass-Radius relationships for solid exoplanets. *ApJ*. **669**, 1279-1297. (DOI 10.1086/521346)
- [8] Grasset, O., Schneider, J. & Sotin, C. 2009 A study of the accuracy of Mass-Radius relationships for silicate-rich and ice-rich planets up to 100 Earth masses. *ApJ*. **693**, 722-733. (DOI 10.1086/0004-637X/693/1/722)
- [9] Adams, E. R., Seager, S. & Elkins-Tanton, L. 2008 Ocean planet or thick atmosphere: On the mass-radius relationship for solid exoplanets with massive atmospheres. *ApJ*. **673**, 1160-1164. (DOI 10.1086/524925)
- [10] Rogers, L. A. & Seager, S. 2010 Three possible origins for the gas layer on GJ 1214b. *ApJ*. **716**, 1208-1216. (DOI 10.088/0004-637X/716/1208)
- [11] Charpinet, S. & 10 co-authors 2011 A compact system of small planets around a former red-giant star. *Nature* **480**, 496-499. (DOI 10.1038/nature10631)
- [12] Morbidelli, A. 2013 Scenarios of giant planet formation and evolution and their impact on the formation of habitable terrestrial planets. *This volume*
- [13] Nelson, R. 2013 The role of migration in planetary system formation. *This volume*
- [14] Vidal-Madjar, A., Lecavelier des Etangs, A., Désert, J.-M., Ballester, G., Ferlet, R., Hébrard, G. & Mayor, M. 2003 An extended upper atmosphere around the extrasolar planet HD209458b. *Nature* **422**, 143-146. (DOI 10.1038/nature01448)
- [15] Vidal-Madjar, A., Lecavelier des Etangs, A., Désert, J.-M., Ballester, G., Ferlet, R., Hébrard, G. & Mayor, M. 2008 Exoplanet HD 209458b (Osiris(1)): Evaporation strengthened. *Astr. J. Lett.* **676**, L57-L60. (DOI 10.1086/587036)
- [16] Erkaev, N.V., Kulikov, Yu N., Lammer, H., Selsis, F., Langmayr, D., Jaritz, G. F. & Biernat, H. K. 2007 Roche lobe effects on the atmospheric loss from "Hot Jupiters". *A&A* **472**, 329-334. (DOI 10.1051/0004-6361:20066929)
- [17] Lecavelier des Etangs, A., Vidal-Madjar, A., McConnell, J. C. & Hébrard, G. 2004 Atmospheric escape from hot Jupiters. *A&A* **418**, L1-L4. (DOI 10.1051/0004-6361:20040106)
- [18] Lecavelier des Etangs, A. 2007 A diagram to determine the evaporation status of extrasolar planets. *A&A* **461**, 1185-1193. (DOI 10.1051/0004-6361:20065014)
- [19] Leitzinger, M. & 12 co-authors 2011 Could CoRoT-7b and Kepler-10b be remnants of evaporated gas or ice giants? *Planet. Space Sci.* **59**, 1472-1481. (DOI 10.1016/j.pss.2011.06.003)
- [20] Steffen, J. H. & 17 co-authors 2013 Transit timing observations from Kepler: VII. Confirmation of 27 planets in 13 multiplanet systems via transit time variations and orbital stability. *Mon. Not. R. Astron. Soc.* **428**, 1077-1087. (DOI 10.1093/mnras/sts090)
- [21] Lithwick, Y., Xie, J. & Yanqin, W. 2012 Extracting planet mass and eccentricity from TTV data. *ApJ*. **761**, 122. (DOI 10.1088/0004-637X/761/2/122)
- [22] Gilliland, R. L., Marcy, G. W. & 32 co-authors 2013 Kepler-68: Three planets, one with a density between that of Earth and ice giants. *ApJ*. **766**, 40. (DOI 10.1088/0004-637X/766/1/40)
- [23] Tian, F., Kasting, J. F., Liu, H.-L. & Roble, R. G. 2008 Hydrodynamic planetary thermosphere model: 1. Response of the Earth's thermosphere to extreme solar EUV conditions and the significance of adiabatic cooling. *J. Geophys. Res.* **113**, E05008. (DOI 10.1029/2007JE002946)
- [24] Yelle, R., Lammer H. & Ip, W.-H. 2008 Aeronomy of extra-solar giant planets. *Space Sci. Rev.* **139**, 437-451. (DOI 10.1007/s11214-008-9420-6)
- [25] Valencia, D., Ikoma, M., Guillot, T. & Nettelmann, N. 2010 Composition and fate of short-period super-Earths. The case of CoRoT-7b. *A&A* **516**, A20. (DOI 10.1051/0004-6361/200912839)
- [26] Stamenkovic, V., Breuer, D. & Spohn, T. 2011 Thermal and transport properties of mantle rock at high pressure: Applications to super-Earths. *Icarus* **216**, 572-596. (DOI 10.1016/j.icarus.2011.09.030)
- [27] Karato, S. 2011 Rheological structure of the mantle of a super-Earth: Some insights from mineral physics. *Icarus* **212**, 14-23. (DOI 10.1016/j.icarus.2010.12.005)

- [28] Lange, R. A. 1994 The effect of H₂O, CO₂, and F on the density and viscosity of silicate melts. *Rev. Mineral.* **30**, 331-369.
- [29] Mookherjee, M., Stixrude, L. & Karki, B. 2008 Hydrous silicate melt at high pressure. *Nature* **452**, 983-986. (DOI 10.1038/nature06918)
- [30] Tackley, P. J., Ammann, M., Brodholt, J. P., Dobson, D. P. & Valencia, D. 2013 Mantle dynamics in super-Earths : Post-perovskite rheology and self-regulation of viscosity. *Icarus* **225**, 50-61. (DOI 10.1016/j.icarus.2013.03.013)
- [31] Dziewonski, A. M. & Anderson, D. L. 1981 Preliminary reference Earth model. *Phys. Earth Planet. Inter.* **25**, 297-356. (DOI 10.106/0031-9201(81)90046-7)
- [32] Peltier, W. R. 1974 The impulse response of a Maxwell Earth. *Rev. Geophys. Space Phys.* **12**, 649-669. (DOI 10.1029/RG012I004p00649)
- [33] Lee, E. H. 1955 Stress analysis in visco-elastic bodies. *Quart. Appl. Math.* **13**, 183.
- [34] Takeuchi, H. & Saito, M. 1972 Seismic surface waves. In *Methods in Computational Physics, vol. 1* (ed. B. A. Bolt), pp. 217-295. New York: Academic Press.
- [35] Tajika, E. 1998 Mantle degassing of major and minor volatile elements during the Earth's history. *Geophys. Res. Lett.* **25**, 3991-3994. (DOI 10.1029/1998GL900106)
- [36] Nettelmann, N., Helled, R., Fortney, J. J. & Redmer, R. 2013 New indication for a dichotomy in the interior structure of Uranus and Neptune from the application of modified shape and rotation data. *Planet. Space Sci.* **77**, 143-151. (DOI 10.1016/j.pss.2012.06.019)
- [37] Saumon, D. & Guillot, T. 2004 Shock compression of Deuterium and the interiors of Jupiter and Saturn. *Amer. Astr. Soc.* **609**, 1170-1180. (DOI 10.1086/421257)
- [38] Muirhead, P. S. & 23 co-authors 2012 Characterizing the cool KOIs. III. KOI 961: A small star with large proper motion and three small planets. *ApJ*. **747**,144. (DOI 10.1088/0004-637X.747/2/144)
- [39] Fressin, F. & 35 co-authors 2012 Two Earth-sized planets orbiting Kepler-20. *Nature* **482**, 195-198. (DOI 10.1038/nature10780)